Systematic investigation of the phase behavior in binary fluid mixtures. II. Calculations based on the Carnahan–Starling–Redlich–Kwong equation of state

Thomas Kraska and Ulrich K. Deiters
Lehrstuhl für Physikalische Chemie II, Ruhr-Universität Bochum, D-4630 Bochum 1, Germany

(Received 10 July 1991; accepted 12 September 1991)

Phase diagrams of binary fluid mixtures have been calculated from the Carnahan–Starling–Redlich–Kwong equation of state in connection with standard quadratic mixing rules. The phase diagrams were classified according to the system of van Konynenburg and Scott and then used to construct global phase diagrams showing the extent of the various phase diagram classes in the space of the parameters of the equation of state. For molecules of equal size, the global phase diagram is rather similar to that of the Redlich–Kwong or the van der Waals equation. For molecules of different sizes, however, a new tricritical line appears. Such a behavior is observed for cubic equations of state only if nonadditive covolumes are assumed. Along this new tricritical line, some unusual phase diagrams involving four-phase states and high-density instabilities can be found. The influence of molecular size ratios on the global phase diagrams and the relationship of the equation of state of this work to the ternary symmetric lattice gas and the van der Waals lattice gas are discussed.

I. INTRODUCTION

During the previous years, the topology of fluid phase diagrams has received increasing scientific interest. While the work of van Konynenburg and Scott[1,2] as well as the work of Furman *et al.*[3] certainly explained the experimentally observed phase equilibrium types and seemed to indicate that—at least for nonpolar binary mixtures—the set of possible fluid phase diagram classes was completely known, recent work has shown that apparently not all possibilities had been exhausted. The prediction of class VI behavior[4,5] (experimentally observed so far only in strongly polar mixtures) as well as the "discovery" of four-phase states in binary mixtures[6] proved that the present understanding of fluid phase diagram classes was not complete. It must be noted, however, that most of the not too numerous systematic investigations of fluid phase diagram topology which had been carried out in the past were concerned mostly with cubic equations of state (e.g., the van der Waals equation[2] and the Redlich–Kwong equation[6]), or models that are analogous to cubic equations (e.g., the van der Waals lattice gas[3] and the symmetric ternary lattice gas[7]). A survey of the literature on fluid phase diagram classification had been given in a previous publication[6]; most of the work on noncubic equations of state published until now is concerned with a rather narrow range of molecular parameters.[8–11] In order to gain some insight into the behavior of noncubic equations of state in phase equilibrium calculations, we have extended our previous work towards the Carnahan–Starling–Redlich–Kwong equation.[12] This equation is one of the simplest possible noncubic equations, but yet useful also for quantitative calculations.

II. EQUATION OF STATE AND MIXING RULES

The Carnahan–Starling–Redlich–Kwong equation (CSRK) is a combination of a hard sphere repulsion term and a Redlich–Kwong attraction term[13]

$$P=\frac{RT}{V_m}\left[1+\frac{4\rho-2\rho^2}{(1-\rho)^3}\right]-\frac{a}{\sqrt{T}\,V_m(V_m+b)},$$
$$\rho=b/4V_m,\quad a=8RT^{*(3/2)}b. \tag{1}$$

The reduced density ρ is calculated from the volume and the van der Waals covolume parameter b. This covolume parameter as well as the attraction parameter of the equation of state are given by quadratic mixing rules

$$a=x_1^2a_{11}+2x_1x_2a_{12}+x_2^2a_{22}, \tag{2}$$
$$b=x_1^2b_{11}+2x_1x_2b_{12}+x_2^2b_{22}. \tag{3}$$

In order to reduce the number of degrees of freedom in our investigation, we define four dimensionless parameter ratios

$$\zeta=\frac{d_{22}-d_{11}}{d_{22}+d_{11}}, \tag{4}$$
$$\lambda=\frac{d_{22}-2d_{12}+d_{11}}{d_{22}+d_{11}}, \tag{5}$$
$$\xi=\frac{b_{22}-b_{11}}{b_{22}+b_{11}}, \tag{6}$$
$$\eta=\frac{b_{22}-2b_{12}+b_{11}}{b_{22}+b_{11}}. \tag{7}$$

The d_{ik} are cohesive energy densities defined by

$$d_{ik}=T_{ik}^{*}(b_{ik}/b_{ii}b_{kk}). \tag{8}$$

For real molecules, the interaction parameters ζ, λ, ξ, and η are not entirely independent of each other, but subject to certain restrictions (combining rules). The following combining rules for the binary interaction parameters (the so-called Berthelot–Lorentz rules) are relatively crude approximations and usually insufficient for the quantitative prediction of phase equilibria, but nevertheless large deviations from these rules are quite unlikely

 0021-9606/92/010539-09$06.00

$$a_{ik} \approx \sqrt{a_{ii} a_{kk}}, \tag{9}$$

$$b_{ik} \approx \tfrac{1}{2}(b_{ii} + b_{kk}). \tag{10}$$

Expressed with relative parameters, these equations become

$$\lambda \approx 1 - [(1-\eta)^2/(1-\xi^2)]^{1/6}(1-\zeta^2)^{1/2}, \tag{11}$$

$$\eta \approx 0. \tag{12}$$

For the phase diagram calculations with the CSRK equation, we have always used $\eta = 0$, hence the mixing rule for b becomes a linear function of composition.

For the calculation of phase diagrams, it is necessary to know the Gibbs or the Helmholtz energy; the latter can be obtained from the equation of state by integration with respect to volume

$$A_m = x_1 A_1^+ + x_2 A_2^+ + RT\left[x_1 \ln x_1 + x_2 \ln x_2 - \ln \frac{V_m}{V_m^+} + \frac{4\rho - 3\rho^2}{(1-\rho)^2}\right] - \frac{a}{b\sqrt{T}} \ln\left(1 + \frac{b}{V_m}\right). \tag{13}$$

A_i^+ denote intrinsic Helmholtz energies of the pure components in the perfect gas state (V_m^+, T). The Gibbs energy is then given by $G_m = A_m + PV_m$.

III. BOUNDARIES BETWEEN PHASE DIAGRAM CLASSES

The various phase diagram classes and the P–T projections of typical phase diagrams have been described in the previous publication. For the reader's convenience, we list the mathematical conditions of the most important boundary states between these classes, namely:

(1) Tricritical states (a three-phase line shrinks to zero length)

$$G_{2x} = G_{3x} = G_{4x} = G_{5x} = 0. \tag{14}$$

G_{kx} is a shorthand notation for $G_{kx} = (\partial^k G_m / \partial x_1^k)_{P,T}$. Phase diagrams with tricritical states form the boundaries between classes II and IV, I and V, or III and IV*.

(2) Double critical endpoints (a critical line touches a three-phase line)

$$G_{2x}^c = G_{3x}^c = 0, \quad \mu_i^c = \mu_i^a, \quad i = 1,2,$$

$$\frac{S_{2x}^c}{V_{2x}^c} = \frac{S_m^c - S_m^a - (x_1^c - x_1^a) S_x^c}{V_m^c - V_m^a - (x_1^c - x_1^a) V_x^c}. \tag{15}$$

Here c denotes the critical phase and a the auxiliary noncritical phase. S_{kx} and V_{kx} are defined in analogy to G_{kx}. Phase diagrams containing double critical endpoints form the boundaries between classes III and IV, or II and IV*.

(3) Zero-temperature endpoints

$$G_{2x} = G_{3x} = 0 \quad \text{at } P, T \to 0. \tag{16}$$

Phase diagrams containing these points form the boundaries between classes I and II, or III and V. Equation (16) depends on the attractive part of the equation of state only; hence the results for the CSRK equation of state are the same as for the original Redlich–Kwong equation.[6]

(4) Azeotropic limits.

The condition of azeotropy is

$$\mu_i^l = \mu_i^g, \quad i = 1,2, \quad x_1^l = x_1^g. \tag{17}$$

For equal-sized molecules, this condition depends on the mixing rule of the attraction parameter only; hence the result is the same as for the Redlich–Kwong equation or the van der Waals equation

$$x_1^{az} = \frac{a_{22} - a_{12}}{a_{11} - 2a_{12} + a_{22}}. \tag{18}$$

The limits of azeotropy, which are specified by $x_1^{az} \to 0$ or $x_1^{az} \to 1$, hence correspond to $\lambda = \pm\zeta$.

(5) Critical azeotropic endpoints (coincidence of a critical endpoint and a critical azeotrope)

$$P_V^c = P_x^c = P_{2V}^c = 0, \quad \mu_i^c = \mu_i^a, \quad i = 1,2. \tag{19}$$

Phase diagrams containing these points form the boundary between the azeotropic class III (III-A) and the heteroazeotropic class III-H.

(In the publication on the phase behavior of the Redlich–Kwong equation, the equation of the azeotropic composition (20)[6] contains a wrong subscript [cf. Eq. (18)]. With the correct equation, the critical azeotropic line of the Redlich–Kwong global phase diagram does not end on a tricritical line, but extends into the shield region as shown in Fig. 1.)

IV. RESULTS FOR THE CSRK EQUATION

For molecules of equal size, the global phase diagram of the CSRK equation (Fig. 1) is very similar to that of the van der Waals or Redlich–Kwong equation of state. Its prominent feature is a set of three tricritical lines, of which two are symmetrical. The third tricritical line coincides with the λ axis. The region around the apparent intersection point (intersection only in the ζ–λ projection), the so-called shield region, contains domains of rather complicated phase diagram classes that have been discussed elsewhere.[2,3] Points where a boundary line terminates for physical reasons (e.g.,

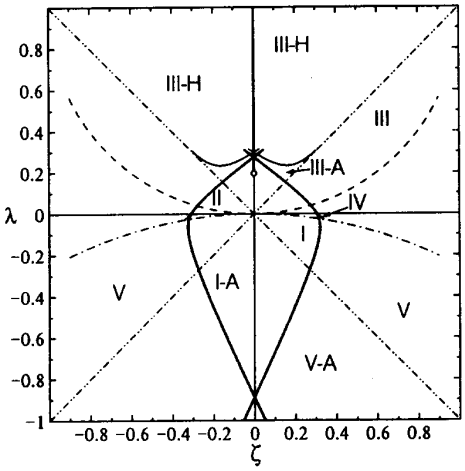

FIG. 1. A global phase diagram of the CSRK equation of state for molecules of equal size ($\xi = 0$, $\eta = 0$)—, tricritical line; ···, its metastable part; – – –, 0 K endpoint curve; – – – –, azeotropic boundary; ---, combining rule (11);—, double or azeotropic critical endpoint curve; O, termination point. Note that the symmetric tricritical line coincides with the ordinate.

pressure becoming zero) have been marked in the diagram. The only topological difference to the global phase diagram of the Redlich–Kwong equation is the behavior of the double critical endpoint line. For cubic equations of state, this line extends into the shield region and intersects the tricritical line in a so-called van Laar point, whereas for the CSRK equation, the double critical endpoint line becomes metastable above $\lambda \approx 0.04$; hence no van Laar point and consequently no domain IV* exist in this diagram. Where the double critical endpoint line is stable, it is so close to the tricritical line that it is almost indistinguishable from it in the global phase diagrams; the domains of class IV are very small.

Even at a relatively small size ratio $\xi = 0.2$, however, departures from this topology are observed (Fig. 2). At the left- and the right-hand sides of the kite-shaped figure containing domains I and II, new tricritical lines appear. Similar behavior is known for the Redlich–Kwong equation of state, but only for larger ξ values, and only for negative ζ values; the tricritical line at positive ζ values has not been observed for cubic equations of state before.

In the phase diagrams of the classes I and V, an additional critical line has been observed at extremely high pressures. This line is a boundary of a high-pressure liquid–liquid immiscibility which extends over a wide temperature range (often beyond the critical temperatures of the less-volatile component). Phase diagram classes with this high-pressure immiscibility have been marked with a superscript "*h*."

The curve with the label "*P*" on the left-hand side of the global phase diagrams represents states which fulfill the criterion for a double critical endpoint, but have a different topology. Instead of merely touching a three-phase line, a critical line intersects this line and the intersection point is an inflection point on the critical line. The *P* line is therefore not a boundary line between different phase diagram classes, but it marks a domain of phase diagrams where the liquid–liquid critical lines have inflection points. The curvature along these critical lines is not large enough to create maxima and minima, but it turns out that other noncubic equations of state exist where such extrema are formed. This would give rise to phase diagram classes VI and VII.[4]

In Fig. 2, the "old" tricritical line, which is also present for equal-sized molecules, runs from the shield region down towards negative λ values; the "new" tricritical line is separate from this line. At still larger size ratios, however, the new tricritical line runs towards the shield region, whereas the low-λ branch of the old tricritical line is now separate (Fig. 3). This change in topology is shown by Fig. 4 in greater detail. On increasing the size ratio ξ, the new tricritical line moves towards the old one, develops a cusp (the section between cusp and endpoint is unstable), and finally switches connections with the old tricritical line. The transition state is a tetracritical point and its thermodynamic conditions are

$$G_{kx} = 0, \quad k = 2,...,7. \tag{20}$$

The coordinates of the tetracritical point are

$$\begin{aligned} &\xi = 0.2552, \quad \eta = 0.0, \quad \zeta = 0.065\,07, \\ &\lambda = -0.037\,98, \quad x_1 = 0.8282. \end{aligned} \tag{21}$$

V. COMPARISON WITH LATTICE-GAS MODELS

A binary fluid mixture obeying the van der Waals equation of state has a Helmholtz energy as follows:

$$A_m^{\mathrm{vdW}} = x_1 A_1^+ + x_2 A_2^+ + RT \times \left(x_1 \ln x_1 + x_2 \ln x_2 - \ln \frac{V_m - b}{V_m^+} \right) - \frac{a}{V_m}. \tag{22}$$

As in Eq. (13), the superscript " + " denotes properties of the thermodynamic reference state.

In lattice-gas theories of binary fluids, volume variations are modeled by introducing vacant sites ("holes") as a third species. There are now three lattice site fractions

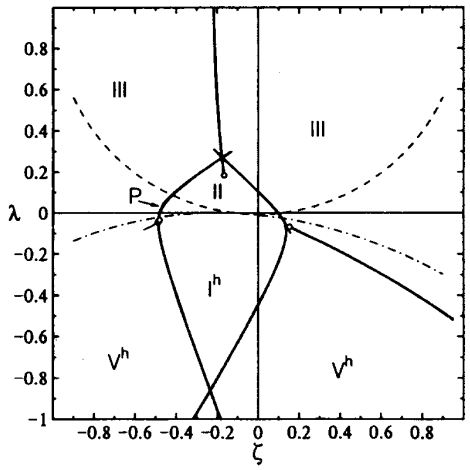

FIG. 2. A global phase diagram of the CSRK equation of state for size ratios $\xi = 0.2$, $\eta = 0$. For an explanation of symbols, see Fig. 1.

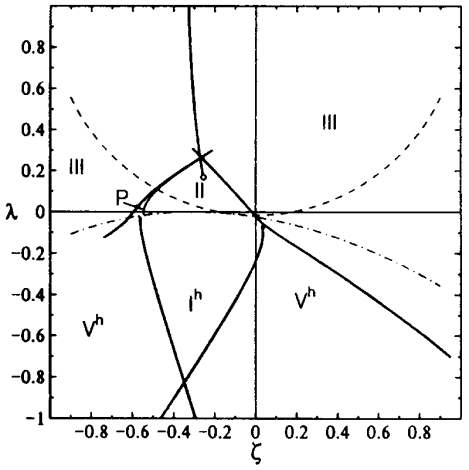

FIG. 3. A global phase diagram of the CSRK equation of state for size ratios $\xi = 0.3$, $\eta = 0$. For an explanation of symbols, see Fig. 1.

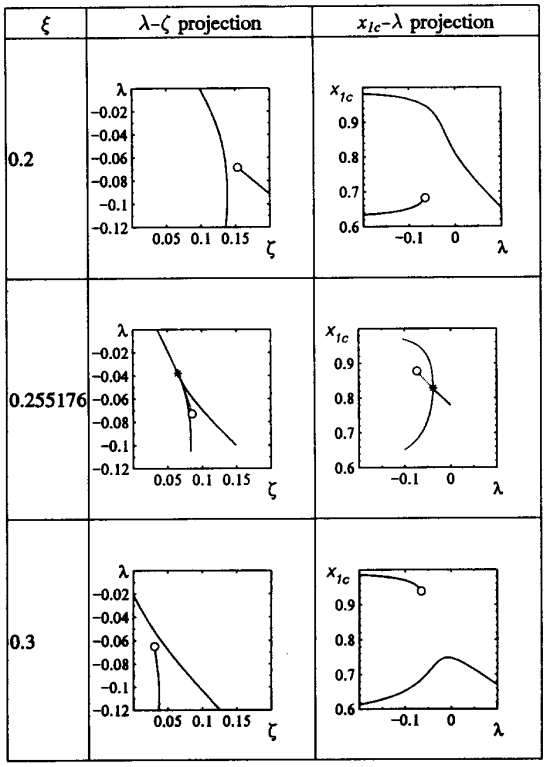

FIG. 4. A tetracritical transition for CSRK mixtures caused by increasing size ratios ξ. For an explanation of symbols, see Fig. 1; the tetracritical point is marked by *.

$$y_i = \frac{x_i b}{V_m}, \quad i = 1,2,$$
$$y_0 = 1 - y_1 - y_2 = 1 - \frac{b}{V_m}. \tag{23}$$

With these new concentration measures, the reduced Helmholtz energy density can be written as

$$F^{\mathrm{vdW}} = \frac{A_m^{\mathrm{vdW}} b}{RTV_m} = \sum_{i=0}^{2} y_i \left(\frac{A_i^+}{RT} - \frac{a_{ii}}{bRT} \right) + y_1 \ln y_1 + y_2 \ln y_2 + (y_0 - 1) \ln y_0 + (y_0 - 1) \times \ln \frac{b}{V_m^+} - \frac{1}{RTb} \sum_{i=0}^{2} \sum_{k<i} y_i y_k (2a_{ik} - a_{ii} - a_{kk}). \tag{24}$$

The parameters A_0^+ and a_{i0}, which denote energy interactions of the holes, are of course zero.

In the case of equal-sized molecules with additive covolumes ($\xi = 0, \eta = 0$), the mixture covolume is a constant, hence all terms containing reference properties are linear functions of y_i and do not have any influence on the phase equilibria. The remaining nonlinear terms correspond to the terms of the van der Waals lattice gas[3]

$$F^{\mathrm{vdWl}} = y_1 \ln y_1 + y_2 \ln y_2 + (y_0 - 1) \ln y_0 + \sum_{i=0}^{2} \sum_{k<i} y_i y_k w_{ik}. \tag{25}$$

The corresponding equation for the ternary symmetric lattice gas is[7]

$$F^{\mathrm{sym}} = y_1 \ln y_1 + y_2 \ln y_2 + y_0 \ln y_0 + \sum_{i=0}^{2} \sum_{k<i} y_i y_k w_{ik}. \tag{26}$$

It is remarkable that the tricritical lines of the ternary symmetric lattice gas, which emerge from the shield region, pass through a tetracritical point and bifurcate. In all the van der Waals models (van der Waals lattice gas, van der Waals fluid, Redlich–Kwong fluid, and CSRK fluid), this tetracritical point does not occur (for equal-sized molecules), and of the two possible branches of the tricritical line, only the one running towards lower λ values is observed. This difference in behavior is attributed to the "loss of symmetry" caused by the transition from the entropy contribution $y_0 \ln y_0$ in Eq. (26) to $(y_0 - 1) \ln y_0$ in Eq. (25).[14]

In order to discuss the influence of size variations, it is advantageous to refer all reduced densities to a fixed covolume parameter, e.g., b_{12},

$$b = \sum_{i=1}^{2} \sum_{k=1}^{2} x_i x_k b_{ik} = b_{12} + (x_1 \Delta_1 + x_2 \Delta_2) - x_1 x_2 (\Delta_1 + \Delta_2)$$
$$\text{with } \Delta_i = b_{ii} - b_{12}, \tag{27}$$

With this notation, the reduced densities can be expressed in terms of concentration-independent covolumes

$$y_i = y_i^* \left(1 + \frac{x_1^2 \Delta_1 + x_2^2 \Delta_2}{b_{12}} \right), \quad i = 1,2,$$
$$y_0^* = 1 - y_1^* - y_2^*. \tag{28}$$

It is now possible to discuss three different cases.

A. van der Waals fluid $\xi \neq 0, \eta = 0$

In this case, the covolume differences are linked by $\Delta_2 = -\Delta_1$ and the reduced densities can be expressed as

$$y_i = y_i^* \left[1 + \frac{\Delta_1 (x_1 - x_2)}{b_{12}} \right] = y_i^* [1 + \xi (x_1 - x_2)], \quad i = 1,2. \tag{29}$$

With the abbreviation

$$\epsilon = \xi (x_1 - x_2), \tag{30}$$

Eq. (24) can be transformed into

$$\frac{F^{\mathrm{vdW}}}{1+\epsilon} = \sum_{i=0}^{2} y_i^* \left(\frac{A_i^+}{RT} - \frac{a_{ii}}{b_{12} RT} \right) + y_1^* \ln y_1^* + y_2^* \ln y_2^* + (y_0^* - 1) \ln y_0^* + (y_0^* - 1) \ln \frac{b_{12}}{V_m^+} + \sum_{i=0}^{2} \sum_{k<i} y_i^* y_k^* w_{ik} + (y_0^* - 1) \ln \frac{y_0}{y_0^*}. \tag{31}$$

This expression differs from Eq. (24) by the last term only, which can be expressed as

$$(y_0^*-1)\ln\frac{y_0}{y_0^*}=(y_0^*-1)\ln\frac{1-(1+\epsilon)(1-y_0^*)}{y_0^*}$$
$$=(y_0^*-1)\ln\left[1+\frac{\epsilon(y_0^*-1)}{y_0^*}\right]$$
$$\approx\frac{(y_0^*-1)^2\epsilon}{y_0^*}\approx\epsilon\ln^2 y_0^*. \tag{32}$$

This additional contribution to F^{vdW} affects the entropic contribution of the hole species

$$\underbrace{(y_0^*-1)\ln y_0^*}_{\text{vdW fluid, const. } b}\rightarrow\underbrace{(y_0^*-1+\epsilon\ln y_0^*)\ln y_0^*}_{\text{vdW fluid, variable } b}\rightarrow\underbrace{y_0^*\ln y_0^*}_{\text{symmetric}}. \tag{33}$$

As $\ln y_0^*$ is always negative, the effect of this additional term depends on the sign of ϵ. This property is not a constant, but a function of composition, but as any new tetracritical point must lie on one of the tricritical lines, it is possible to restrict the discussion to the range of mole fractions that occur along the tricritical line. For positive values of ξ (species 2 larger than species 1) two cases must be distinguished:

$\zeta>0$—the tricritical mode fraction in the vicinity of the ζ axis and below is above 0.8; hence ϵ is positive. The additional term moves the van der Waals model *away* from the symmetric lattice gas model. Additional tricritical lines are suppressed.

$\zeta<0$—the tricritical mole fraction in the vicinity of the ζ axis and below is below 0.2; hence ϵ is negative. The additional term moves the van der Waals model *towards* the symmetric lattice gas model. Additional tricritical lines are made possible.

The argumentation is not quite rigorous, because the additional term depends on composition and therefore leads to further contributions to higher derivatives of the Gibbs energy. Nevertheless, it is made plausible why the additional tricritical lines can appear and why this takes place for negative values of ζ only.

B. van der Waals fluid $\xi=0$, $\eta\neq0$

In this case, $\Delta_2=+\Delta_1$, hence the reduced densities can be written as

$$y_i=y_i^*[1+(\Delta_1/b_{12})(x_1^2+x_2^2)]$$
$$=y_i^*[1+2\eta(x_1^2+x_2^2)]. \tag{34}$$

Evidently, this case can be reduced to the previous case by redefining

$$\epsilon=2\eta(x_1^2+x_2^2). \tag{35}$$

As the term in parentheses is always positive, only the sign of η determines the possibility of additional tricritical lines. The existence of tetracritical points and the branching of tricritical lines is possible for negative values of η only, but if it occurs, it can be found for $\zeta>0$ as well as for $\zeta<0$.

C. Carnahan–Starling–van der Waals fluid $\xi\neq0$, $\eta=0$

The repulsive term of the van der Waals equation of state is given by

$$Z_{\mathrm{rep}}^{\mathrm{vdW}}=\frac{V_m}{V_m-b}=1+\frac{4\rho}{1-4\rho}, \tag{36}$$

where ρ is defined as in Eq. (1). This can be rewritten with reduced densities related to b_{12} by means of Eqs. (29) and (30)

$$Z_{\mathrm{rep}}^{\mathrm{vdW}}=1+\frac{4(1+\epsilon)\rho^*}{1-4(1+\epsilon)\rho^*}. \tag{37}$$

On the other hand, it is possible to expand the Carnahan–Starling hard-sphere equation around the van der Waals repulsion function

$$Z^{\mathrm{CS}}=1+\frac{4\rho-2\rho^2}{(1-\rho)^3}$$
$$\approx1+\frac{4\rho}{1-4\rho}\left(1-\frac{3}{2}\rho-\frac{11}{2}\rho^2-11\rho^3\cdots\right). \tag{38}$$

Setting $\rho=(1+\epsilon')\rho^*$ in this equation and equating $Z^{\mathrm{CS}}=Z_{\mathrm{rep}}^{\mathrm{vdW}}$ leads to

$$1+\epsilon=\frac{(1+\epsilon')[1-\frac{3}{2}\rho^*(1+\epsilon')-\frac{11}{2}\rho^{*2}(1+\epsilon')^2-\cdots]}{1-6\rho^{*2}(1+\epsilon')^2-22\rho^{*3}(1+\epsilon')^3-\cdots}. \tag{39}$$

The evaluation of this expression to first order yields

$$\epsilon\approx\epsilon'-\tfrac{3}{2}\rho^*(1+\epsilon')^2+\cdots. \tag{40}$$

The leading additional term in this equation is always negative, regardless of the sign of ϵ'. Switching from the van der Waals to the Carnahan–Starling repulsion function is therefore equivalent to using more negative ϵ in the perturbed van der Waals lattice-gas model [Eq. (31)] and this again implies a shift towards the symmetric lattice-gas model [Eq. (26)]. This explains the appearing of new tricritical lines on both sides of the global phase diagram.

Equation (40) can also be written as

$$\epsilon\approx\epsilon'-3\rho^*(1+\epsilon')^2(x_1^2+x_2^2)+\tfrac{3}{2}\rho^*(1+\epsilon')^2$$
$$\times(x_1-x_2)^2+\cdots. \tag{41}$$

Comparison with Eq. (35) shows that the Carnahan–Starling hard-sphere equation with $\eta=0$ behaves approximately like the van der Waals repulsion function with $\eta=-3\rho^*(1+\epsilon')^2$, i.e., with binary covolume b_{12} which is *larger* than the arithmetic mean of the pure component covolumes.

The above considerations refer to the van der Waals equation of state, or to related equations containing the van der Waals attraction term, but it is possible to generalize the results to the CSRK equation. The conditions of tricritical states [Eq. (14)] do not contain derivatives of the Gibbs energy with respect to temperature, hence the pattern of tricritical lines is not affected by the temperature dependence of the attraction term.[15] Furthermore, the substitution of V_m^2, the denominator of the van der Waals attraction term, by $V_m(V_m+b)$ does not lead to large deviations in the density range considered; the global phase diagram of the Redlich–Kwong equation of state is merely a distorted version of the global phase diagram of the van der Waals equation.[6]

VI. SYSTEMS WITH NONADDITIVE COVOLUMES

In the previous section, a new tricritical line has been predicted for van der Waals type equations of state with nonadditive covolumes, which should occur for positive ξ values. This has caused us to calculate the global phase diagram for a symmetric Redlich–Kwong mixture with $\xi = 0$, $\eta = -0.05$.

Even with this small departure from covolume additivity, the global phase diagram (Fig. 5) already shows a pattern of tricritical lines similar to Fig. 3, thus confirming the prediction.

Because of the new tricritical line, the boundary between classes III and V can no longer be a line of 0 K endpoints. In order to determine the true nature of the transition from class III to V, we have calculated a series of phase diagrams in the vicinity of this tricritical line. The results are shown in Fig. 6 not only as P–T projections, but also—following a recommendation of Meijer *et al.*[14,16]—as $y_1 - y_2$ density plots. The latter representation helps to understand the connectivity of the critical lines. For this purpose, the metastable and unstable portions of the critical lines are also shown.

In all P–T diagrams in Fig. 6, the critical line originating at the critical point of component 1 covers a very small temperature range, before it becomes metastable and—passing through a cusp—unstable. In the projection, the critical endpoint on this critical line almost coincides with the pure fluid critical point and its three-phase line is practically indistinguishable from the vapor pressure line. In the Meijer diagrams, this critical line runs from the pure fluid critical point towards the lower right corner and practically coincides with the diagram abscissa.

The new tricritical curve marks the transition from class III to IV*. For a phase diagram on this boundary, the high-pressure three-phase line has zero length and its endpoints coincide, thus forming a tricritical point.

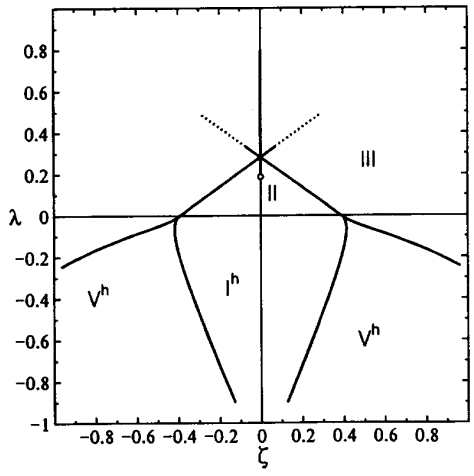

FIG. 5. A global phase diagram of the Redlich–Kwong equation of state for molecules of equal size with nonadditive covolumes ($\xi = 0$, $\eta = -0.05$). For an explanation of symbols, see Fig. 1. Note that the symmetric tricritical line coincides with the ordinate.

It must be noted that the connectivity of the critical lines changes within class IV*. The transition state, where the two cusps of the critical lines meet, is a mathematical double point and as such is unstable. This changeover of critical line branches would not be accessible to experiments.

The Meijer diagrams of the class IV* reveal that the whole phase diagram contains *three* different critical lines. This is unusual, because until now all common phase diagram classes of binary fluid mixtures could be represented by *two* different critical lines. (To the experimentalist, class IV has three critical lines, but the calculation always shows that two of them are joined by metastable or unstable sections and hence must be counted as one line only.)

The phase diagrams of the symmetric ternary lattice gas contain six unique critical points:

three stable critical points (corresponding to the pure fluid critical points and the "jamming point" C_m at high pressure). These points are found on the sides of the Meijer triangle;

three unstable critical points (corresponding to $T = 0$, $P = 0$ or similar "impossible" limiting states). These points are represented by the corners of the Meijer diagram.

As there are six points to choose from, it is possible to construct up to three critical lines between them. The appearance of a third critical line for the binary fluid mixtures studies in this work is further proof of our view that fluid mixtures with $\xi > 0$ or $\eta < 0$ are intermediates between the van der Waals ternary lattice gas and the symmetric ternary lattice gas. We note, however, that in the Meijer diagrams for the CSRK equation, more than one critical line can end in a corner, while another corner has no critical line.

If λ is decreased further, the critical endpoints of the liquid–liquid critical lines approach the liquid–liquid–gas three-phase line. For a small range of λ values, this leads to the formation of four-phase states (class IV_4). The transition from class IV* to IV_4 is characterized by phase diagrams containing a critical phase coexisting with two noncritical ones (BA_2 in the Griffiths nomenclature[7]). For still lower λ values, class IV occurs. In contrast to the "usual" class IV, however, the high-pressure critical line is not an extension of the critical line originating at the critical point of component 2. Furthermore, it does not run towards the jamming point any more, but seems to form a loop in the Meijer diagram. It is possible for this distorted class IV to have the three-phase lines share the same temperature range.

A typical $T - x_1$ phase diagram for this case is shown schematically in Fig. 7. This diagram also applies to phase diagrams of class IV_4 slightly above the four-phase state, if the lower critical endpoint (on the critical line originating at the critical point of the less volatile compound) has a *lower* pressure than the four-phase state. Otherwise, three three-phase lines run from the four-phase point upwards and the resulting isobaric phase diagram is represented schematically by Fig. 8. A remarkable feature of this phase diagram is a homogeneous domain (labeled "l_2") in the midst of the two-phase regions.

Finally, the phase behavior looks like class V. However, the liquid–liquid immiscibility at extremely high pressures (> 5 GPa) persists. This is a natural consequence of having

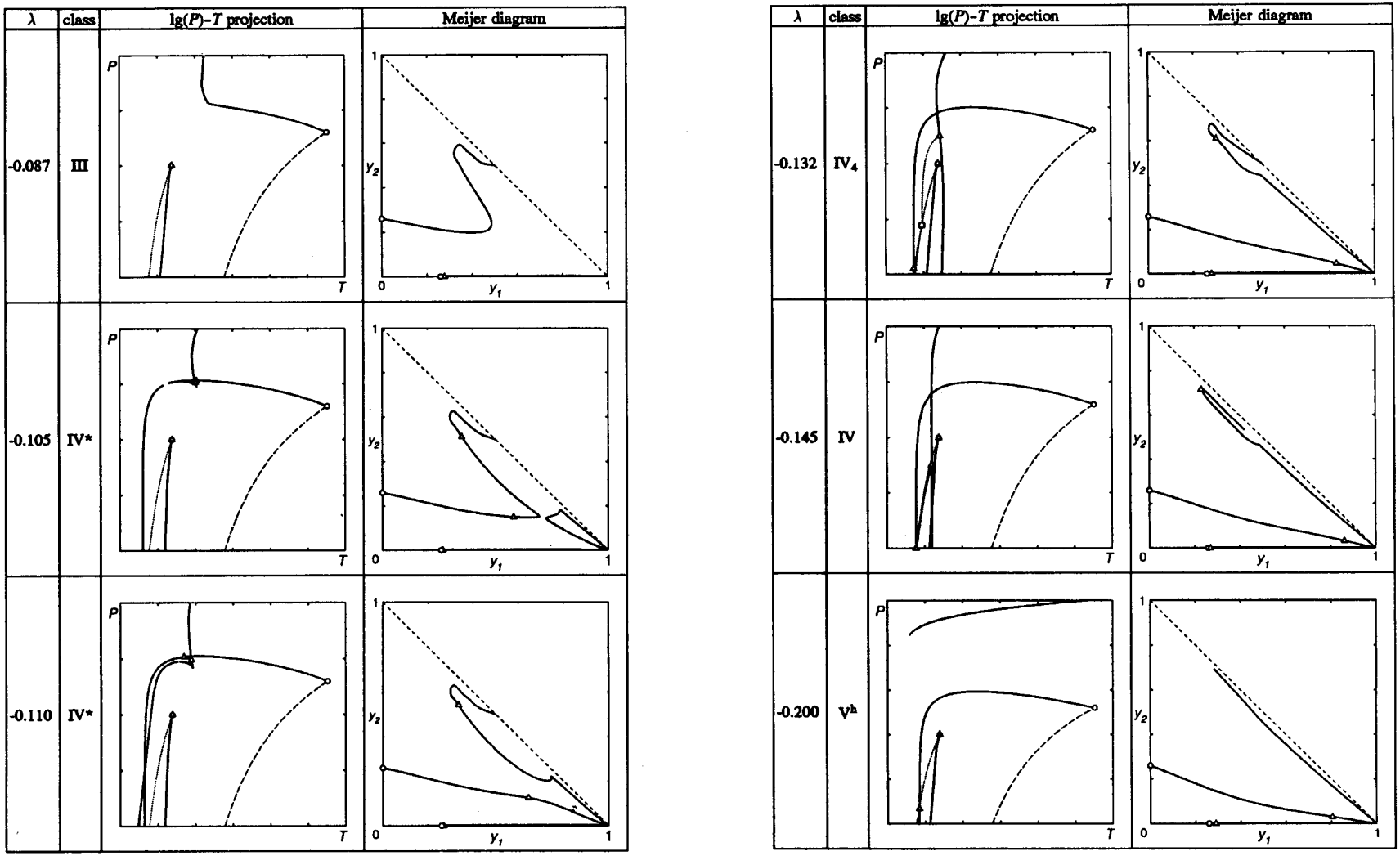

FIG. 6. Phase diagrams of Redlich–Kwong mixtures with $\xi = 0$, $\eta = -0.05$, $\zeta = 0.6$ for various λ values. —, critical line; ---, vapor pressure line; ···, three-phase line; ○, pure component critical point; △, endpoint.

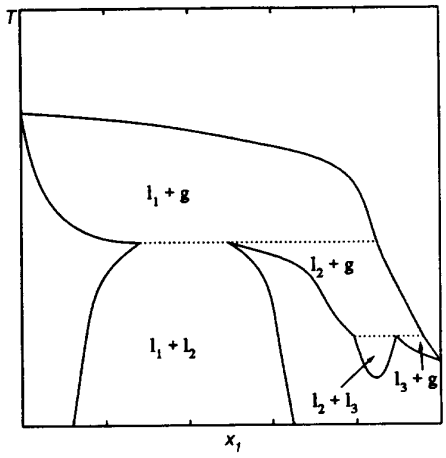

FIG. 7. A schematic isobaric phase diagram for a "reversed" class IV (cf. Fig. 6, $\lambda = -0.145$) in the pressure range where two three-phase lines occur, or for class IV_4 (cf. Fig. 6, $\lambda = -0.132$) at a pressure slightly above the four-phase state.

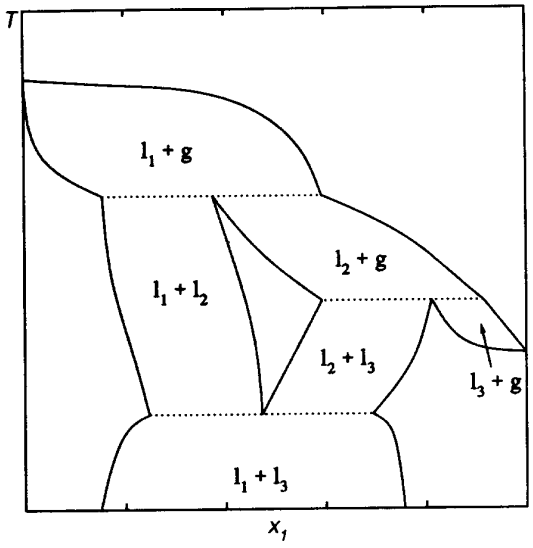

FIG. 8. An alternative schematic isobaric phase diagram for class IV_4 at a pressure slightly above the four-phase state.

a negative η. The mixture covolume is larger than the arithmetic mean of the pure component covolumes and therefore a sufficiently high pressure will always enforce demixing. Since the CSRK equation shows similar phase behavior as the Redlich–Kwong equation with negative η, this explains the high-pressure immiscibility mentioned in Fig. 2.

For still more negative η values, the high pressure immiscibility would extend to lower pressures and perhaps interact with the usual liquid–gas phase equilibria, thus creating new phase diagram classes. It is possible that this is the reason for some unusual phase diagrams obtained with the simplified perturbed hard chain theory (SPHCT) equation, which contains a modified Carnahan–Starling function.[5]

VII. DISCUSSION

In the previous sections, the interaction parameters ζ, λ, ξ, and η have been treated as independent variables. Since with real molecules, deviations from the combining rules (9) and (10) of more than 20% would be rather exceptional, it has been concluded[17] that it will not be possible to find a real system with a sufficiently high λ value to belong to the shield region. It must be noted, however, that the parameter range into which the shield region falls depends on the equation of state. For equal-sized molecules, the λ parameter for the center of the shield region is approximately 0.44 for the van der Waals equation of state, 0.34 for the Redlich–Kwong equation, and 0.29 for the CSRK equation. One might conclude that the more realistic the equation of state is, the lower the shield region will be. Therefore, the task of finding an experimental binary system belonging to the shield region classes II*, III*, or III** might not be hopeless after all.

Another interesting, but rather speculative feature of this work is the prediction of phase diagram classes with four-phase states. Such states are predicted for mixtures having either negative η parameters or large size ratios ξ. While the global phase diagrams for the CSRK equation contain two domains of phase diagram class IV_4, the cubic equations (with $\eta = 0$) have only one. This region occurs at very negative ζ values and at values of the binary interaction parameter λ, which are close to the abscissa. Such λ values would be far below the values calculated from the combining rules (9) and (10), and hence might be considered unrealistic.

There is, however, a case in which the Berthelot–Lorentz combining rules would be inappropriate. In a microscopically heterogeneous fluid, the quadratic mixing rules (2) and (3) would have to be replaced by linear ones. For the energy parameter, this would be equivalent to replacing the geometric mean in the combining rule by the arithmetic mean and this would indeed lead to $\lambda \approx 0$. Therefore, an appropriate binary system to show class IV_4 behavior should meet the following requirements:

(1) its first component should have a high critical pressure and a small molecular volume (e.g., water);

(2) its other component should have a low critical pressure and a large molecular volume and either interact extremely favorably with the other component (e.g., a long-chain polyether); or

(3) the mixture should form micelles.

An interesting candidate for class IV_4 behavior might be the system (water + 3,6,9,12-tetraoxadocosanol). Its second component is a nonionic surfactant ("$C_{10}E_4$"). In this binary system, a three-phase state has been observed experimentally, where three *liquid* phases coexist.[18] The experiments had been carried out at ambient or slightly elevated pressure; lowering the pressure towards the vapor pressure of water would certainly have brought about a four-phase state (three liquid + one vapor phase). Until now, only a small part of the phase diagram of this binary mixture is known and it is not entirely clear to which phase diagram class it belongs, but at least the practical existence of fluid four-phase states is made certain. Furthermore, these results indi-

cate that equations of state can at least describe qualitatively the phase behavior of oil–surfactant–water mixtures.

ACKNOWLEDGMENTS

The authors wish to thank Paul H. E. Meijer (Catholic University of America, Washington, D.C.) for fruitful discussions. Financial support by the Deutsche Forschungsgemeinschaft and by the Fonds der Chemischen Industrie e. V. is gratefully acknowledged. One of us (U. K. D.) has received a stipend from the Karl-Winnacker-Stiftung.

[1] R. L. Scott and P. H. van Konynenburg, Discuss. Faraday Soc. **49**, 87 (1970).
[2] P. H. van Konynenburg and R. L. Scott, Philos. Trans. R. Soc. London Ser. A **298**, 495 (1980).
[3] D. Furman and R. B. Griffiths, Phys. Rev. A **17**, 1139 (1978).
[4] L. Z. Boshkov, Dokl. Akad. Nauk SSSR **294**, 901 (1987).
[5] A. van Pelt, C. J. Peters, and J. de Swaan Arons, J. Chem. Phys. (to be published).
[6] U. K. Deiters and I. L. Pegg, J. Chem. Phys. **90**, 6632 (1989).
[7] D. Furman, S. Dattagupta, and R. B. Griffiths, Phys. Rev. B **15**, 441 (1977).
[8] I. L. Pegg, C. M. Knobler, and R. L. Scott, J. Chem. Phys. **92**, 5442 (1990).
[9] G. Jackson, J. S. Rowlinson, and C. A. Leng, J. Chem. Soc. Faraday Trans. I **82**, 3461 (1986).
[10] P. Clancy, K. E. Gubbins, and C. G. Gray, Discuss. Faraday Soc. **66**, 116 (1978).
[11] L. Z. Boshkov and V. A. Mazur, Russ. J. Phys. Chem. **60**, 16 (1986).
[12] Th. Kraska, diploma thesis, Ruhr-Universität Bochum, 1988.
[13] N. F. Carnahan and K. E. Starling, AIChE. J. **18**, 1184 (1972).
[14] P. H. E. Meijer, M. Keskin, and I. L. Pegg, J. Chem. Phys. **88**, 1976 (1988).
[15] A. Bolz, diploma thesis, Ruhr-Universität Bochum, 1989.
[16] P. H. E. Meijer and M. Napiórkowski, J. Chem. Phys. **86**, 5771 (1987).
[17] I.-C. Wei and R. L. Scott, J. Stat. Phys. **52**, 1315 (1988).
[18] J. C. Lang and R. D. Morgan, J. Chem. Phys. **73**, 5849 (1980).